16A.2 RE-CREATION OF HISTORIC IOWA EF-5 TORNADO ENVIRONMENTS USING HIGH-RESOLUTION WORKSTATION WRF OUTPUT INITIALIZED WITH NCEP REANALYSIS GRIDS

Karl Jungbluth *
National Weather Service, Des Moines, Iowa

1. INTRODUCTION

The most damaging of tornadoes, the EF-5, requires a unique combination of synoptic scale pattern and near-storm environment in order to occur. Even though tornadoes occur every year in Iowa and the upper Midwest, tornado outbreaks, especially those producing EF-4 or EF-5 damage*, are rare. This limits forecaster experience with the mesoscale environments that produce high-end tornado events. Although there is an understanding of the basic synoptic scale patterns (Figs. 1 and 2), forecasters do not have much first-hand knowledge of the mesoscale and near-storm environment associated with Iowa's most violent tornadoes. This is especially true when one considers the evolution of "modern" severe weather tools such as CAPE, 0-1km shear, LCL heights and proximity soundings in the hours just before the tornadoes occurred.

A number of disastrous EF-5 tornadoes occurred in Iowa in the days before real-time mesoanalysis and high resolution numerical models made it possible to get a comprehensive understanding of their near-storm environment. In addition, much has been learned about the environmental conditions most relevant to high-end tornado development since these events occurred, and since associated studies were undertaken, if any studies were conducted at all. Example cases include the EF-5 Jordan, Iowa tornado on 13 June 1976 and the Charles City, Iowa tornado on 15 May 1968.

1.1 *Hypothesis*

This paper explores the utility of using short-range, high-resolution workstation Weather Research and Forecasting model (WRF) output to paint a picture of the mesoscale conditions which preceded a number of EF-5 tornado events. To expand the dataset, six tornado outbreaks that included an EF-4 tornado were also added. *It is hypothesized that one can "zoom in" on the mesoscale environments of historic violent tornadoes, by starting with a large-scale initial dataset and running progressively higher resolution nests of the WRF model.* This approach has been utilized to a limited extent by other authors, most notably Locatelli et al. (2002) for the 3-4 April 1974 super outbreak.

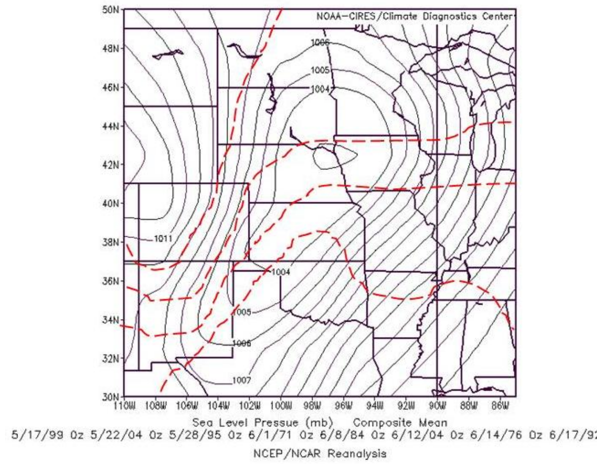

Figure 1: NCEP/NCAR Reanalysis composite of surface pressure and temperature (dashed red) for 12 of Iowa's most damaging warm season tornado outbreaks since 1950. Courtesy of Craig Cogil, NWS Des Moines.

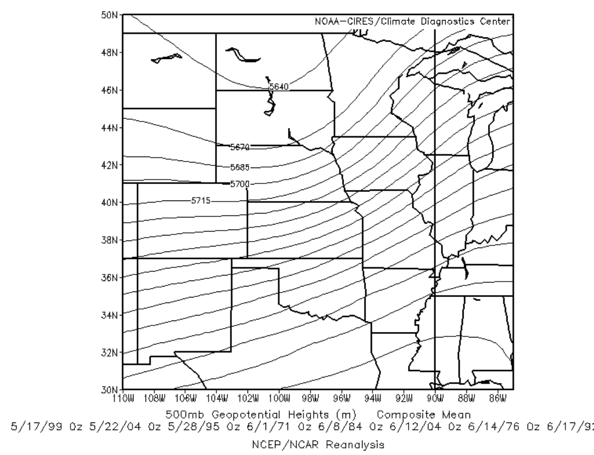

Figure 2: NCEP/NCAR Reanalysis composite of 500-mb heights for twelve of Iowa's most damaging warm season tornado outbreaks since 1950. Courtesy of Craig Cogil, NWS Des Moines.

For this research, NCEP reanalysis grids on two scales are used for initialization of the WRF model. Output from eleven cases is analyzed in much the same way that forecasters approach looking at a severe storm environment today, with emphasis upon instability and shear parameters in various layers. A small subset of those parameters is shown here. In addition, basic WRF output fields such as mean sea level pressure and

* *Corresponding author address:* Karl Jungbluth, National Weather Service - Des Moines, 9607 NW Beaver Drive, Johnston, IA 50131; e-mail: Karl.A.Jungbluth@noaa.gov.

* EF-scale is referenced for both recent and historical tornadoes because EF-scale, and the original F-scale ratings, are the same. The difference is in the estimated wind speed ranges for each scale (WSEC 2006).

500-hPa heights are compared to historical analyses, serving as a double check to ensure that WRF output has produced a reasonable synoptic scale solution, e.g., one that can be downscaled to approximate the mesoscale severe storm environment.

This downscaling approach has its dangers. A basic WRF-EMS (WRF Environmental Modeling System; NWS 2006) configuration is used here, but different horizontal or vertical resolutions, different physics schemes, or different model domains could produce different, better or worse results. Gallus and Bresch (2006), Aligo et al. (2008), Jankov et al. (2005) and others have shown that lateral boundary conditions, physical parameterization schemes and vertical grid resolution all impact warm season rainfall simulations. Warner and Hsu (2000) showed that coarse-grid parameterized convection has large impacts on simulated explicit convective precipitation from finer domain simulations, a factor if nested runs are to be used. Weisman et al. (2008), utilizing the Advanced Research WRF (ARW; Skamarock et al. 2005) at 4-km resolution along with explicit convective forecasts, found improved structure and evolution of mesoscale phenomena, but little improvement over coarser simulations in the location or timing of convective systems.

With that in mind, section 2 of this paper describes initialization datasets and the configuration of the WRF-EMS used for this research, and briefly discusses sensitivity studies conducted for two of the EF-5 events. Section 3 shows WRF results, both compared to large-scale reanalysis of surface and upper air-charts, and on a finer mesoscale approach. Section 4 comprises lessons learned about the merits of this approach, and also summarizes the environments of Iowa's EF-5 tornadoes. Finally, section 5 sites broader conclusions and desires for future work.

2. METHOD, MODEL CONFIGURATION AND INITIALIZATION DATA SETS

When this study began, there had been four EF-5 tornado days in Iowa since 1950, with none since 1976. That number grew to five, with the addition of the Parkersburg/New Hartford EF-5 tornado on 25 May 2008 (Marshall et al. 2008). All were modeled. In addition, six EF-4 tornado days were modeled, with the intent to expand the dataset and to include more cases since 1979, when higher resolution North American Regional Reanalysis (NARR) initialization data is available. Days with noteworthy EF-4 tornadoes, and relatively higher destruction potential index (DPI; Thompson and Vescio, 1998) were chosen. See Table 1.

In general, the WRF-EMS model was initialized at 1200 UTC, and run for a 12-hour or 15-hour simulation. The WRF-ARW core was used for all runs, along with the Lin et al. (1983) microphysical scheme. Kain-Fritsch (1993) convective parameterization was used for all domains or nests with 8-km or greater grid resolution. No convective scheme was used at 5-km or below. Two-way nesting was employed, allowing feedback from each nested domain to its parent domain at each time step. All of the historical EF-4/5 tornadoes occurred between 2000 UTC and 0200 UTC, allowing 8 to 14 hours of spin up time in the numerical model before tornadoes would have occurred.

TABLE 1

Date	Tornado Time	Rating	Location
6/27/1953	21 UTC	EF-5	Rural Cass-Adair counties
10/14/1966	20 UTC	EF-5	Belmond
5/15/1968	21-22 UTC	EF-5	Charles City - Oelwein
6/18/1974	02-03 UTC	EF-4	Ankeny
6/13/1976	21 UTC	EF-5	Jordan
6/28/1979	23-0030 UTC	EF-4	Manson - Algona
6/7/1984	23–02 UTC,	EF-4	Decatur-Mahaska counties, Barnaveld, WI
5/27/1995	23-00 UTC	EF-4	Carroll - Creston
5/24/1989	22-23 UTC	EF-4	Prescott + Marshall county
4/8/1999	20-21 UTC	EF-4	Carbon
5/25/2008	22-23 UTC	EF-5	Parkersburg-New Hartford

Cases prior to 1979 were initialized with NNRP data, which are available at a 6-hour time interval, and on roughly a 210-km horizontal resolution (Kistler et al. 2001). Achieving realistic mesoscale results from this spatially and temporally course data set proved to be a challenge, especially for the most weakly forced EF-5 tornado day, 13 June 1976. As a result, a number of test runs were completed in search of a configuration that could produce an overall reasonable prediction in a subjective sense. Trials included a variety of nested domains and single domains, and several grid resolutions from 90-km down to 2.5-km. Results indicated that at domains/nests from 30-km grid spacing down to 10-km, parameterized convection dominated where it occurred, and it often produced unrealistically large convective outflows that overspread large regions. For weaker-forced cases, these outflows contaminated later hours and finer scale nested solutions.

For example, a 32-10.6-3.5 km nested run initialized at 1200 UTC on 13 June 1976 developed convection in all nests over north-central-Missouri. See Figure 3. Omega fields at 900-mb (Fig. 4, on domain 2) illustrate how this convection produced extreme and unrealistic outflows between 1800 and 2100 UTC, rendering the simulation unusable. Results were similar for all nested runs at a number of grid scales and different sized domains. Interestingly, a run configured the same as the example above, except initiated at 1800 UTC, produced convection over Iowa (closer to reality), and not over Missouri (Fig. 5). This convection also did not produce the wild scale of outflow like the 1200 UTC run, for reasons that are not known to this author.

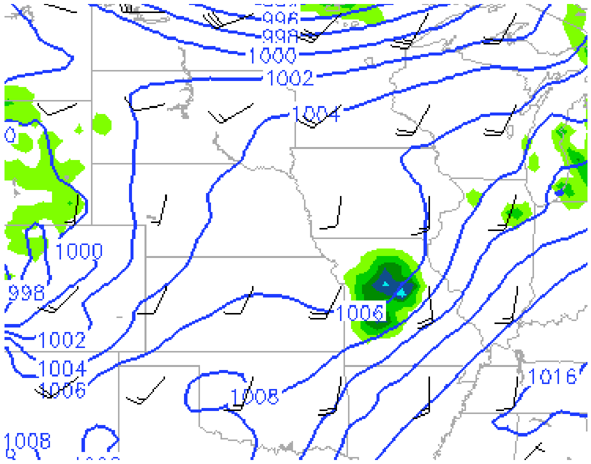

Figure 3. Domain 1, 6-hr forecast valid at 1800 UTC 13 June 1976 32-km WRF MSLP/surface wind (kt) and 1-hr precip. The size of the domain was much larger than this image, from eastern Kentucky to California.

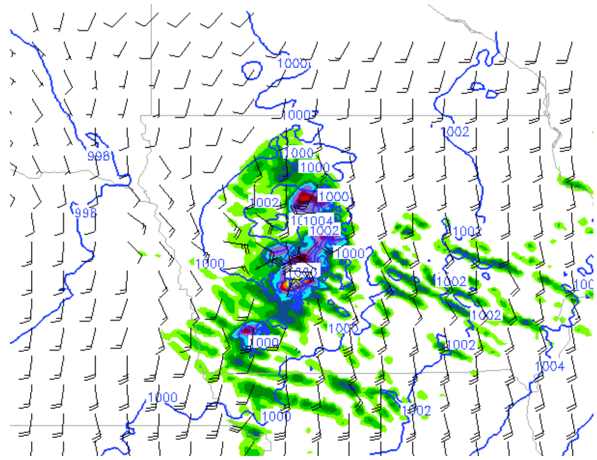

Figure 5. Domain 3, 6-hr forecast valid at 0000 UTC 14 June 1976 3.5-km WRF MSLP/surface wind (kt) and 1-hr precip. The size of the domain was near the size of this image.

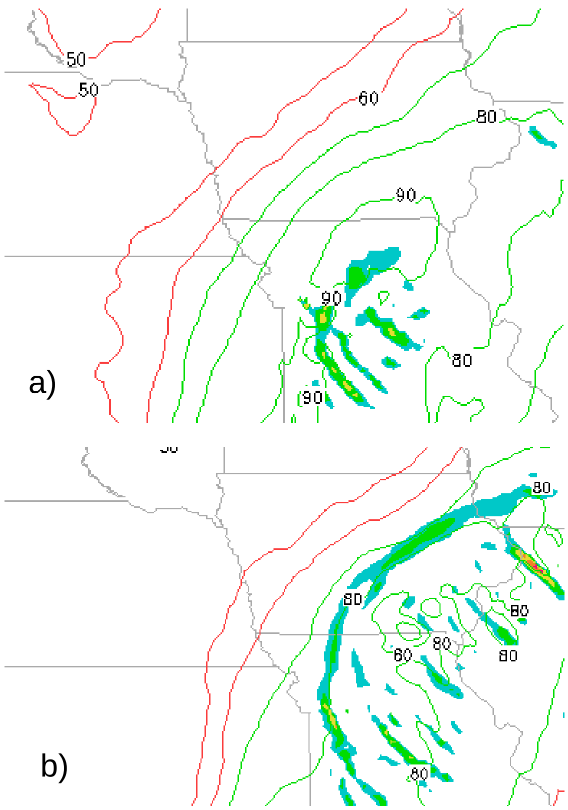

Figure 4. Domain 2 a) 6-hr forecast valid at 1800 UTC 13 June 1976 10.6-km WRF 900-mb relative humidity (contours and labels) and omega (shaded, Pa/s) . b) Same as 2a, but at 9-hr forecast valid at 2100 UTC. The size of the domain was also much larger than this image.

Single domain runs were also attempted at fairly high resolution from 12-2.5 km. Even when initialized straight from the course global reanalysis (NNRP) grid, they apparently did not exhibit negative effects from domain boundary transition problems, *except* at finer resolution and with smaller domains. In those cases, analysis of 925-mb UVV showed waves of upward motion originating at the edge of the domain and propagating northeastward with the mean flow. For the 13 June 1976 case, this spurious vertical motion (Fig. 6a) was seen to initiate convection within the instability maxima during the afternoon hours (Fig. 6b), the location of which changed geographically depending upon where the edge of the domain was located. For example, Figure 7 shows the results when the southern boundary of the domain was moved farther south. The convection developed 2-3 hours earlier than in the more northern domain, and it had a different, less organized character.

In the end, it was determined that a fairly large single domain 12-km grid produced more realistic pre-storm environmental conditions for the most cases. This domain stretched from east Lake Superior on the northeast to the Baja Peninsula on the southwest. With this configuration, negative effects of parameterized convection (from the nested runs) and domain boundary effects (from the single domain high-resolution runs) were less of a factor. This selection seems to go against conventional modeling wisdom (personal communication with a number of scientists) that running a high-resolution domain which is initialized by a very low-resolution dataset will ultimately shock the system and produce undesirable results. However, it worked for these short 12-15 hour runs. Results may not be as attractive for longer 24-36 hour runs.

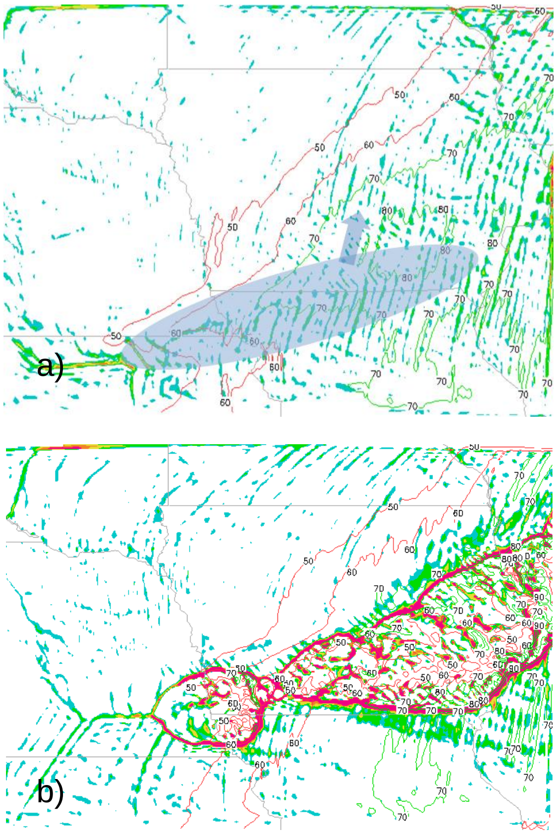

Figure 6. Full domain view at a) 2000 UTC 13 June 1976 2.5-km WRF 900-mb relative humidity (contours and labels) and omega (shaded, Pa s^{-1}), Blue shaded area is axis of spurious upward vertical velocity that is believed to have originated at the southern domain edge earlier in the simulation. b) Same as 6a, but at 2300 UTC.

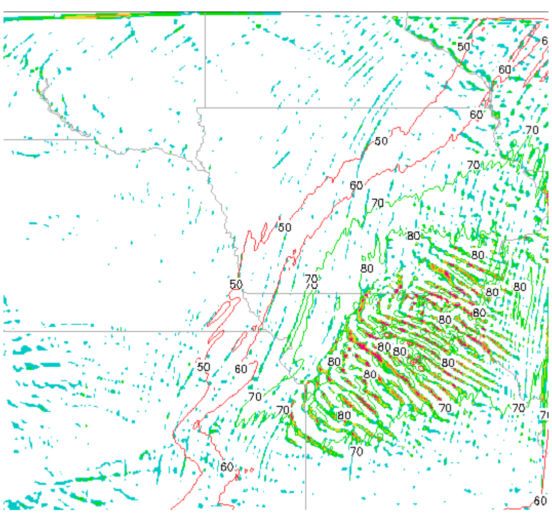

Figure 7. Full domain view 6-hr forecast valid at 2000 UTC 13 June 1976 2.5-km WRF 900-mb relative humidity (contours and labels) and omega (shaded, Pa s^{-1}). Note the difference in convective character when compared to Figure 6b. Both were approximately 3 hours after convection developed in the WRF simulation.

For cases from 1979 on, NARR data (Mesinger 2006) was utilized for initialization. NARR data are available at 32-km resolution and a 3-hour time step. Model configuration was the same as for the pre-1979 date, except that a nested domain of 32-11-3.5 km was used for all runs. Kain-Fritsch convective parameterization was used for the 32 and 11-km domains, with no convective scheme at 3.5-km. As might be expected, model results were more consistent when initiated with this higher temporal and spatial data set.

3. RESULTS

Model output is now shared for all five of the EF-5 Iowa tornado events, and one of the EF-4 events. Comparative analysis data is also provided, although this information is by no means exhaustive. Thanks to Jonathan Finch for allowing use of analysis graphics for comparison to model results. Similar analyses can be found at bangladeshtornaodoes.org. Synoptic scale NCEP/NCAR reanalysis charts, for comparison to WRF output, are provided by the NOAA/ESRL Physical Sciences Division, Boulder Colorado from their Web site at http://www.cdc.noaa.gov/.

3.1 *27 June 1953 EF-5*

This was the same year as the famous Worcester, Massachusetts EF-4 tornado, and no towns were hit in Iowa, so information is sketchy. The 10 mile long tornado passed 4 miles south of the town of Adair at around 2045 UTC. (Fig. 8)

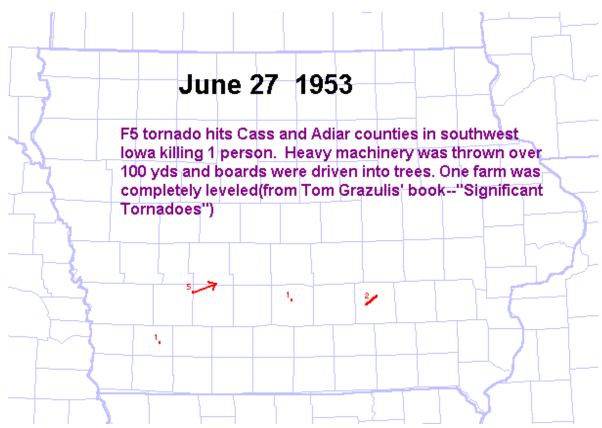

Figure 8. Plot of tornadoes on 27 June 1953 from SPC SeverePlot program. Courtesy of Jonathan Finch.

A comparison of 500-mb heights at 00 UTC 28 June 1953 shows reasonable agreement between the large-scale reanalysis (Fig 9a) and the 12-km WRF output valid at the same time (Fig 9b). The WRF output shows effects of convection from central Iowa into Wisconsin, otherwise the heights and gradients are similar.

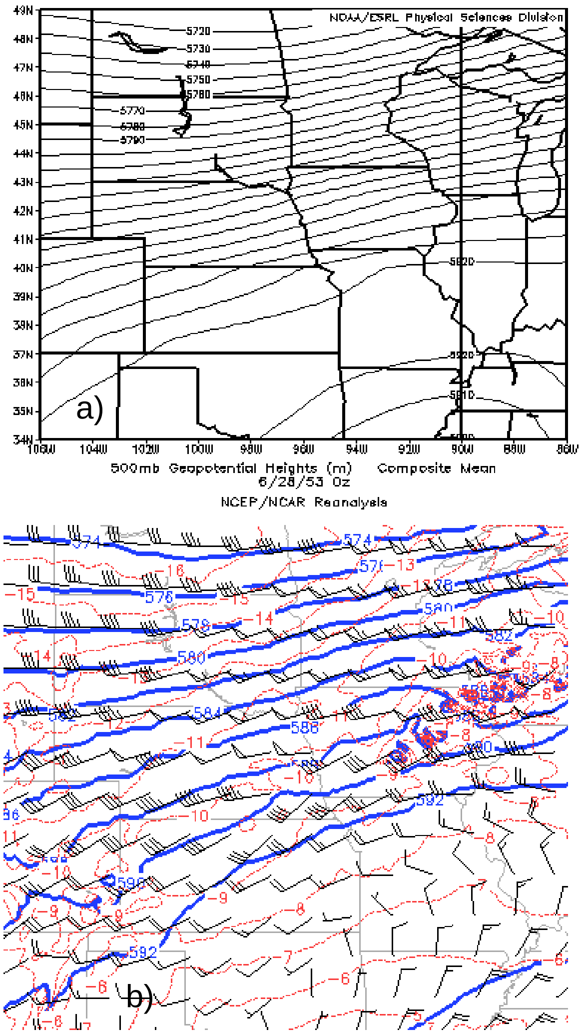

Figure 9. a) Reanalysis 500-mb height at 00 UTC 28 June 1953. b) 12-km WRF output - 500mb height/temp/wind 12-hr forecast valid at the same time.

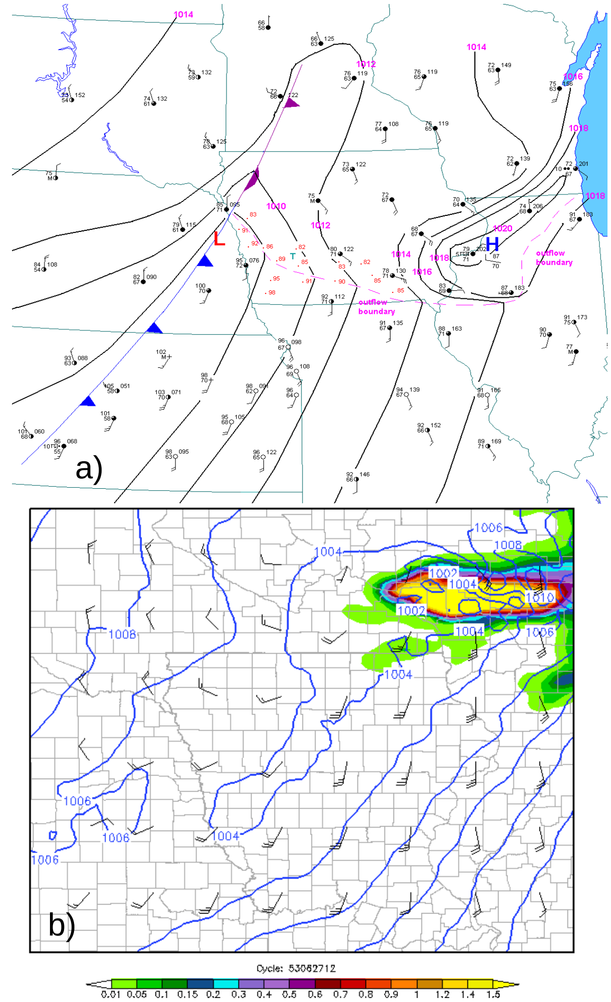

Figure 10. a) 2030 UTC hand-plotted and analyzed surface map (courtesy Jonathan Finch). Maximum temperatures from cooperative observers are plotted in red. B) 9-hr forecast 2100 UTC 27 June 1953 12-km WRF MSLP/surface wind (kt) and 1-hr precip.

Figure 10 compares a hand-plotted and analyzed surface map (courtesy Jonathan Finch) to the WRF output. The WRF surface pressure trough appears too far east of the surface wind shift line in the model, and too far east of the hand surface analysis. The low pressure center in southern Minnesota also appears overdone, and there is obviously no evidence of backed surface winds in south-central Iowa, which are the result of a convective outflow boundary. This feature, if it can be correlated at all to reality, occurs over Wisconsin and southeast Minnesota in the WRF. Still, wind fields and conditions in the warm sector near the Iowa/Missouri border do not seem unreasonable.

CAPE values from the WRF were extreme over central Iowa. The axis of CAPE expanded rapidly northward between 1800 and 2200 UTC, with values exceeding 5000 J kg^{-1} at 2100 UTC (Figure 11). Again, there is no evidence of a WNW-ESE CAPE gradient that would have been present in central Iowa based upon the surface observations.

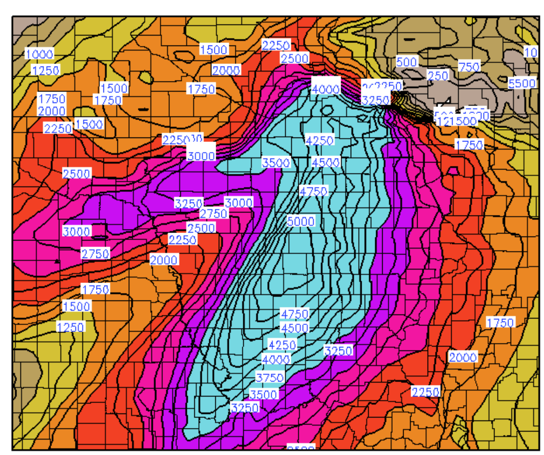

Figure 11. Surface-based CAPE (J kg^{-1}) from the 12-km WRF 9-hr forecast valid at 2100 UTC 27 June 1953.

WRF 0-1 km bulk shear values were extreme at 1200 UTC on 27 June 1953, in excess of 50 kt (26 ms^{-1}), but these values decreased markedly near the tornado location as the maximum moved northeast during the day. At 2100 UTC, values still exceeded 30 kt (15 ms^{-1}) in central Iowa, but were much less (10 kt, 5 ms^{-1}) farther west at the specific tornado location (Figure 12). 0-3 km storm-relative helicity (SRH) was around 100 m^2s^{-2} at 2100 UTC near Adair, but the maximum values were much farther east in the WRF, from east-central Iowa into Wisconsin.

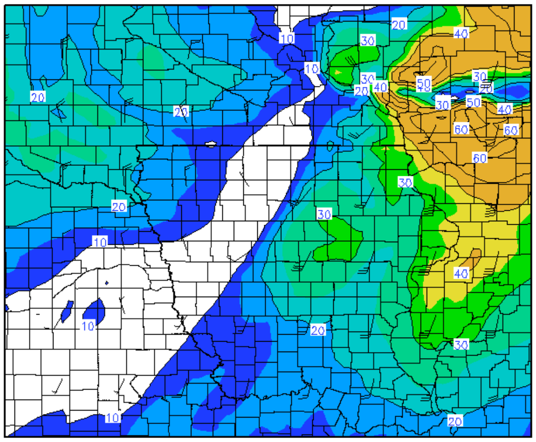

Figure 12. 9-hr forecast valid at 2100 UTC 27 June 1953 12-km WRF 0-1 km shear magnitude and vector (kt).

A WRF forecast sounding for Des Moines (DSM), which is 50 miles east of the actual tornado location, is shown in Figure 13. This sounding is representative of the environment ahead of the cold front in the WRF simulation. Obvious features are the extremely steep mid-level lapse rates, from 700 to 400-mb, extreme instability, moderate deep-layer shear and strong curvature in the 0-3 km hodograph plot. Forecast storm motion looks reasonable compared to the actual tornado track. Once again, this sounding does not reflect the low-level rain-cooled air and backed surface wind flow shown in the surface conditions in Figure 12 over DSM.

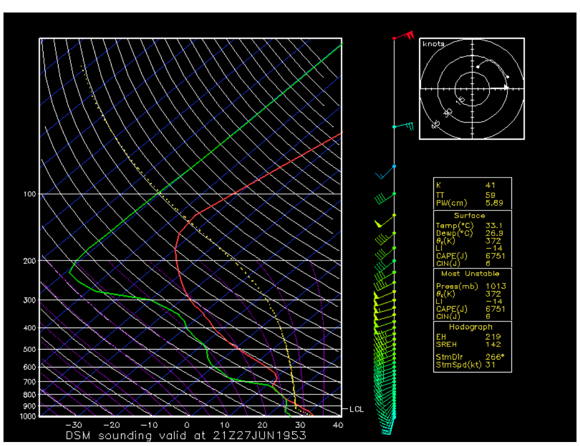

Figure 13. 9-hr forecast sounding valid at 2100 UTC 27 June 1953 for DSM.

3.2 *14 October 1966 Belmond, IA EF-5*

The Belmond tornado was part of a much larger outbreak that extended well south into Missouri (Figure 14). It is Iowa's most famous fall tornado. The tornado had a 12 mile path, and destroyed many farms in addition to businesses in Belmond. Photos in electronic format are difficult to come by. Figure 15 is one example.

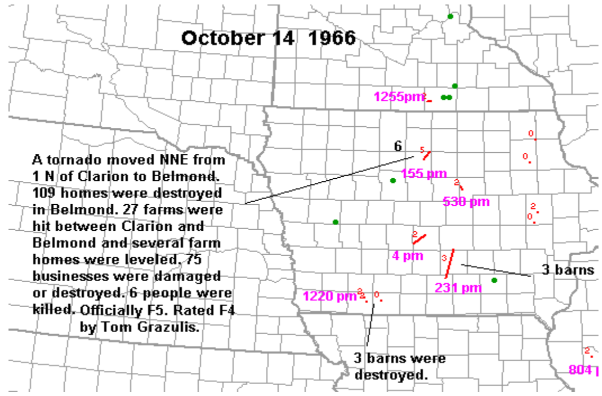

Figure 14. Plot of tornadoes on 14 October 1966 from SPC SeverePlot program. Courtesy of Jonathan Finch.

Figure 15. Downtown Belmond, Iowa after the tornado. Globe Gazette file photo.

A comparison of 500-mb heights at 0000 UTC 15 October 1966 shows reasonable agreement between the large-scale reanalysis (Fig 16a) and the 12-km WRF output at the same time (Fig 16b). The WRF output exhibits a slightly sharper axis to the 500-mb trough, but the 500-mb gradient is properly located from Oklahoma into Missouri and eastern Iowa.

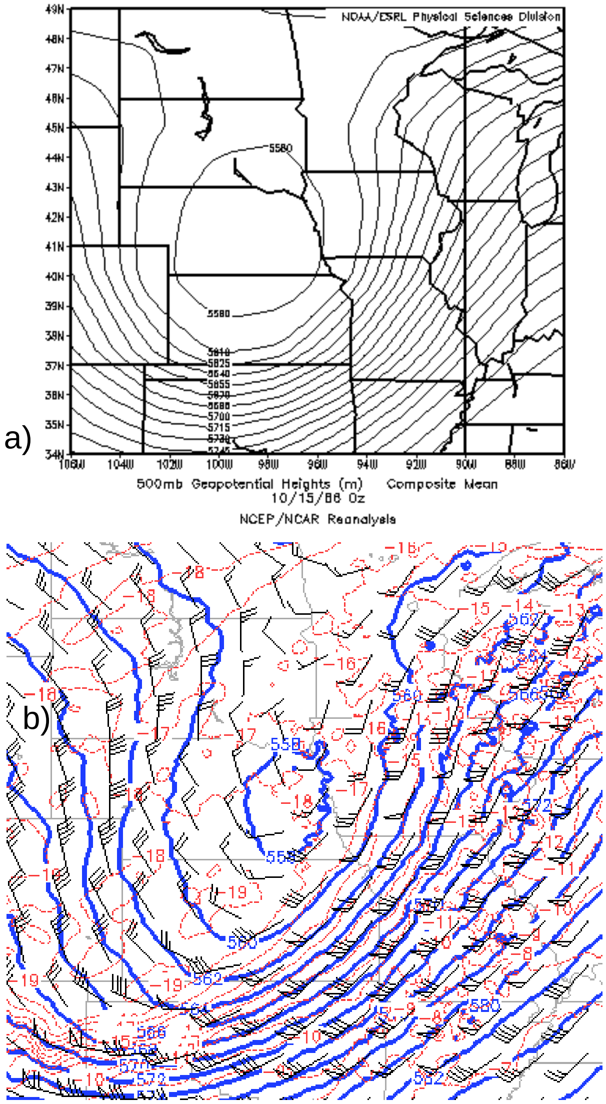

Figure 16. a) Reanalysis 500-mb height at 00 UTC 15 October 1966. b) 12-hr forecast 12-km WRF output - 500mb height/temp/wind valid at the same time.

Figure 17 compares a hand-plotted and analyzed surface map (courtesy Jonathan Finch) to the WRF output. The WRF surface low pressure center compares well to the hand analysis, although the low center is slightly farther east. The pressure and wind fields also highlight some of the double pressure trough structure in the hand analysis over Kansas, but again this feature is somewhat farther east. Despite a good pressure depiction, backed (SSE) surface flow is not present in the WRF surface winds over northeast Iowa and southeast Minnesota.

Note that by 2200 UTC, the WRF generates a number of strong, isolated areas of convection (Fig. 18) that is reflected in 1-hourly precipitation output (Fig. 19). This hints at proper convective structure and location relative to the actual tornado occurrence, but it is unknown (and possibly unlikely) that the results would be reproducible, especially given this is a 12-km simulation.

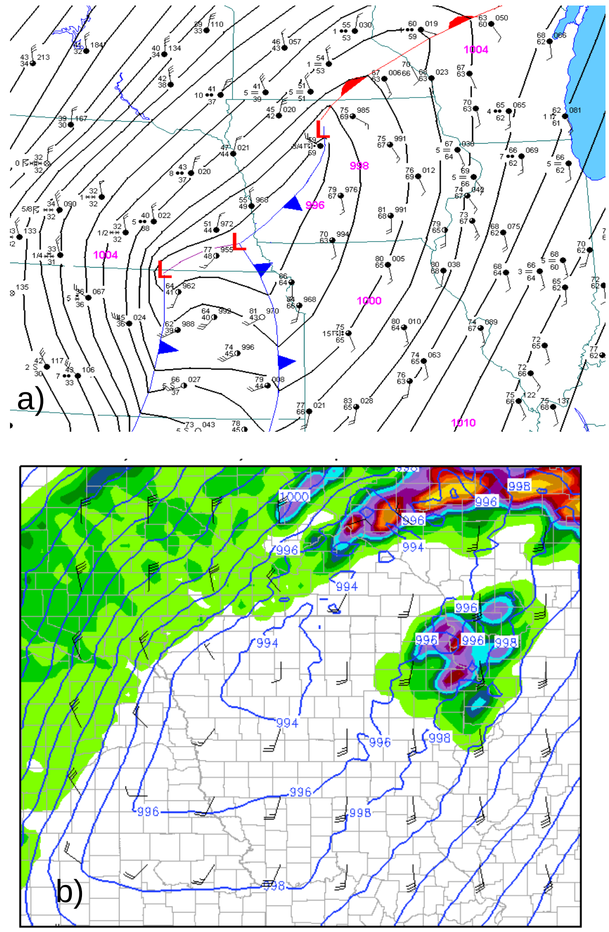

Figure 17. a) 2000 UTC 14 October 1966 hand-plotted and analyzed surface map (courtesy Jonathan Finch). B) 8-hr forecast valid at 2000 UTC14 October 1966 12-km WRF MSLP/surface wind (kt) and 1-hr precip.

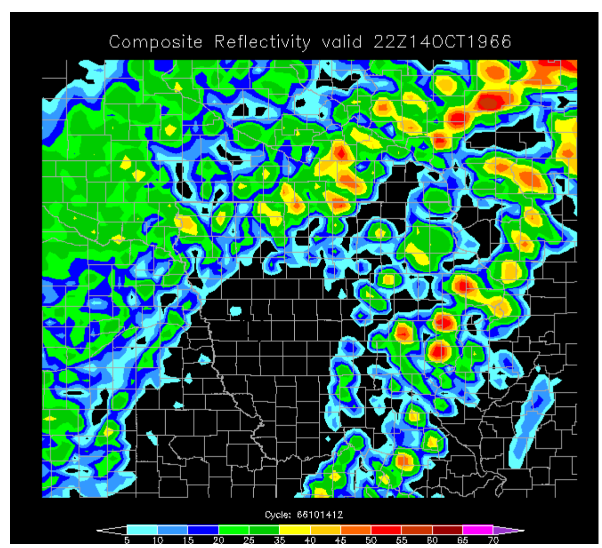

Figure 18. 2200 UTC WRF model simulated composite radar reflectivity.

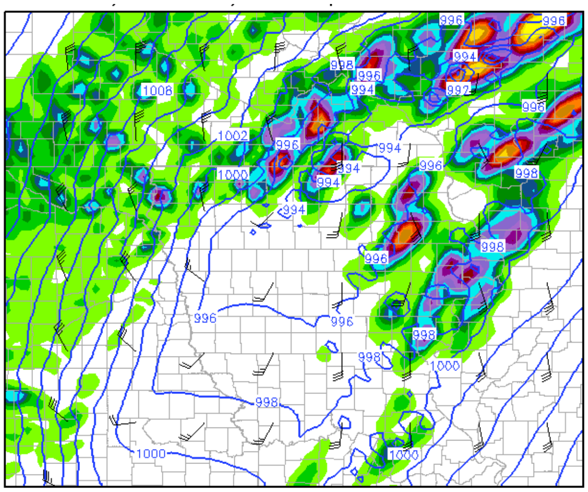

Figure 19. 10-hr forecast valid at 2200 UTC WRF simulated 1-hr precipitation (shaded).

CAPE values from the WRF exceeded 2700 J kg^{-1} over north-central Iowa by 2100 UTC (Fig. 20). The north-south axis of CAPE expanded northward during the preceding 6-hours, with the maximum values in close proximity to the Belmond tornado location. These values look realistic when compared to the 2000 UTC surface plot (Fig. 17a).

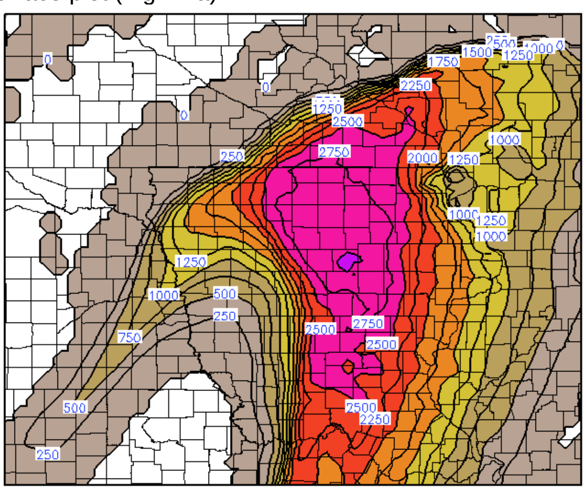

Figure 20. Surface-based CAPE (J kg^{-1}) from the 12-km WRF. 8-hr forecast valid at 2000 UTC 14 October 1966.

WRF 0-1 km bulk shear values were in excess of 40 kt over the eastern half of Iowa before 1800 UTC on 14 October 1966. These values tailed off somewhat by 2000 UTC (Fig. 21), but were still moderately strong at around 30 kt (21 ms^{-1}). Actual values, with backed SSE surface flow (Fig. 17a) could have been stronger. Values from the WRF were much stronger farther east over eastern Iowa into Illinois and Wisconsin, at greater than 50 kt (26 ms^{-1}).

A WRF forecast sounding for Mason City (MCW; Fig. 22) was chosen as a representative location, 20 miles northeast of the tornado location in Belmond. Obvious features are the steep full tropospheric lapse rates, strong instability, moderate deep-layer speed shear but limited directional shear. Forecast storm motion looks reasonable compared to the actual tornado track, although it has a slightly more westerly component than observed. Once again, this sounding does not reflect the backed surface wind flow shown in the surface conditions in Figure 17a over northern and northeast Iowa.

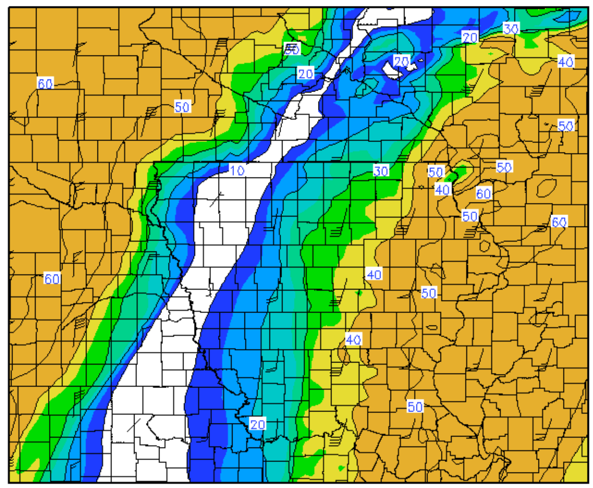

Figure 21. 8-hr forecast valid at 2000 UTC 14 October 1966 12-km WRF 0-1 km shear magnitude and vector (kt).

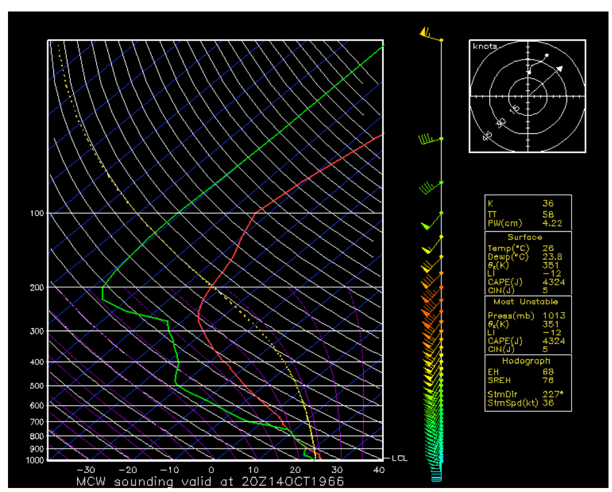

Figure 22. 8-hr forecast sounding valid at 2000 UTC 14 October 1966 MCW.

3.3 *15 May 1968 Charles City, IA EF-5*

Not one, but two EF-5 tornadoes occurred on 15 May 1968. The Charles City tornado (Fig. 23) was followed in less than one hour by an EF-5 tornado in Oelwein to produce Iowa's most deadly and destructive tornado outbreak in the past 100 years. Thirteen people were killed in Charles City and 5 died in Oelwein. The tornadoes had 65 mile and 15 mile tracks, respectively (Fig. 24), and were part of a huge outbreak of tornadoes that included an EF-4 tornado in Arkansas.

Figure 23. Photo of the Charles City tornado when it was 2 miles southwest of town, taken by the Floyd County sheriff (L. L. Lane) (A special thanks to Mark Wicks from The Charles City Press who provided this photo for use on the NWS La Crosse, WI website.)

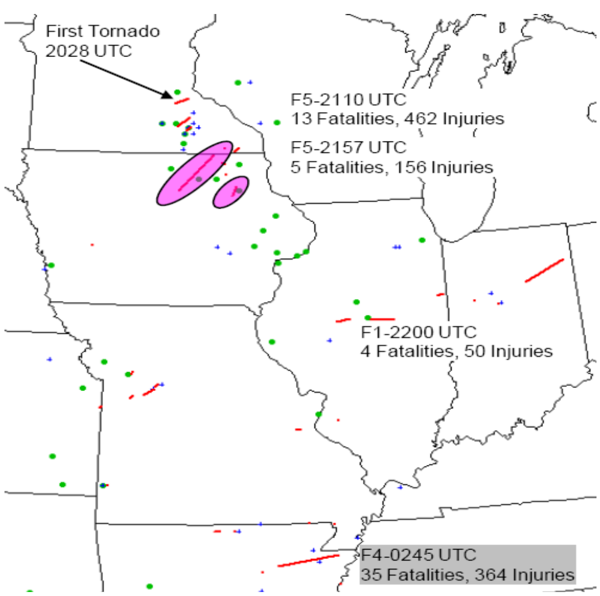

Figure 24. Plot of tornadoes on 15 May 1968 from SPC SeverePlot program. The Charles City tornado is the northwestern track (highlighted in pink), and the Oelwein tornado is just southeast. Courtesy of Greg Carbin, SPC.

The 500-mb heights at 0000 UTC 16 May 1968 are indicative of a strong and progressive shortwave trough in the middle troposphere. There is good agreement between the large-scale reanalysis (Fig 25a) and the 12-km WRF output at the same time (Fig 25b). Feedback from parameterized convection is apparent over MN/WI/IL in Figure 25b.

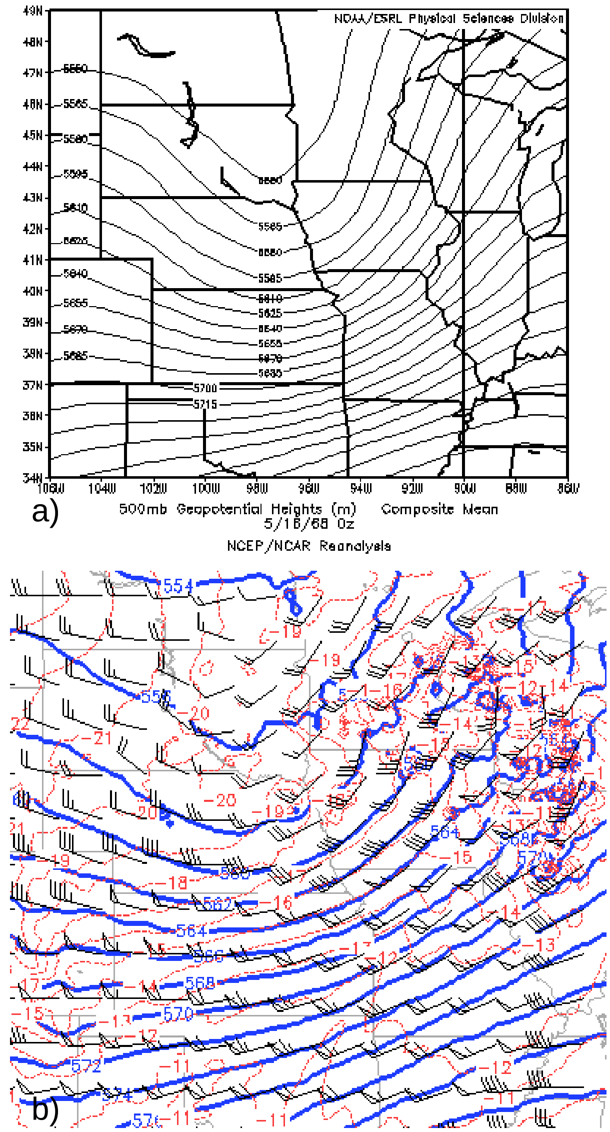

Figure 25. a) Reanalysis 500-mb height at 00 UTC 16 May 1968. b) 12-hr forecast 12-km WRF output - 500mb height/temp/wind valid at the same time.

Figure 26 compares a hand-plotted and analyzed surface map (courtesy Jonathan Finch) to the WRF output. Agreement between the two is quite striking, with the exception of the outflow boundary and ESE surface winds over southeast Iowa into Illinois. This appears to be a case, based upon Figures 25 and 26, where confidence could be placed in the WRF mesoanalysis fields. However, the WRF is not producing any precipitation at 2000 UTC when an EF-5 tornado was occurring in northern Iowa. By 2200 UTC, the simulation looks more accurate (Fig. 27). WRF precipitation from 22-2300 UTC (Figure 28) also looks plausible for a simulation at 12-km resolution, albeit a couple of hours late and too far to the east.

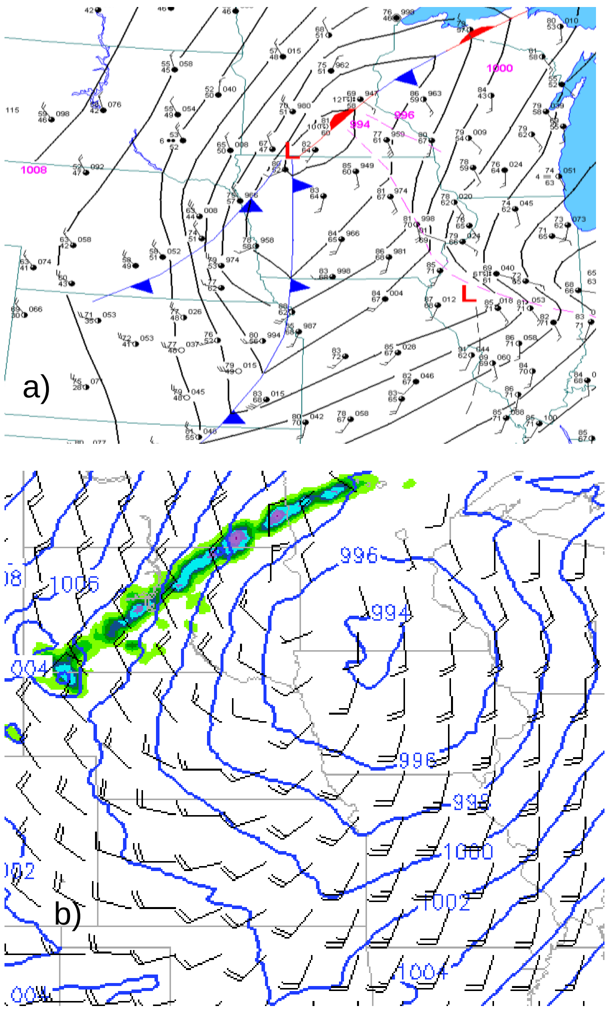

Figure 26. a) 2000 UTC 15 May 1968 hand-plotted and analyzed surface map (courtesy Jonathan Finch). b) 8-hr forecast valid at 2000 UTC 15 May 1968 12-km WRF MSLP/surface wind (kt) and 1-hr precip.

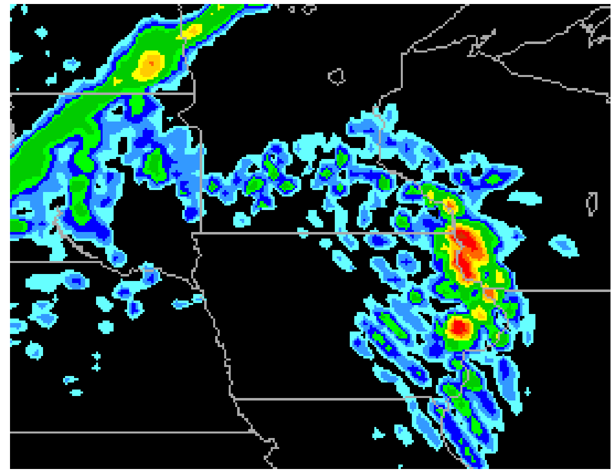

Figure 27. 8-hr forecast 2200 UTC 15 May 1968 WRF model simulated composite radar reflectivity.

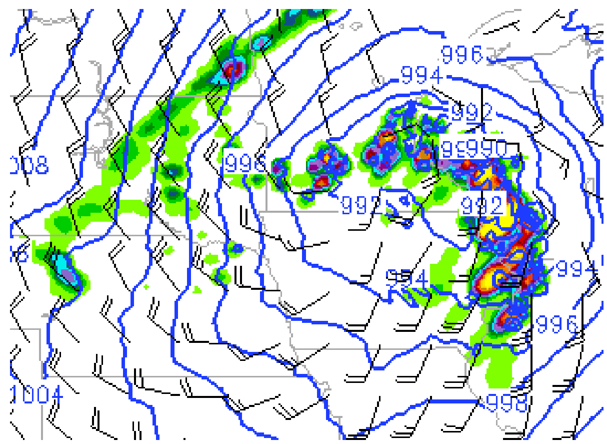

Figure 28. 11-hr forecast valid at 2300 UTC WRF simulated 1-hr precipitation (shaded).

The maximum of WRF CAPE roared northward from eastern Oklahoma into eastern Iowa during the day. Values of surface-based CAPE from the WRF exceeded 3700 J kg^{-1} over eastern Iowa by 2100 UTC (Fig. 29) and these values look realistic when compared to the 2000 UTC surface plot (Fig. 26a).

WRF 0-1 km bulk shear climbed during the morning hours and maintained 25-30 kt (14 ms^{-1}) values over the eastern half of Iowa during the afternoon of 15 May 1968 (Figure 30).

The WRF forecast sounding for Charles City (CCY; Fig. 31) again shows steep full tropospheric lapse rates, strong instability, moderate deep-layer speed shear and weak to moderate directional shear.

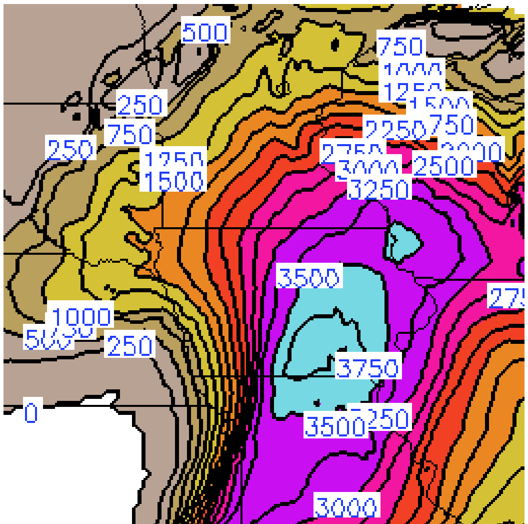

Figure 29. 8-hr forecast surface-based CAPE (J kg^{-1}) from the 12-km WRF valid at 2000 UTC 15 May 1968.

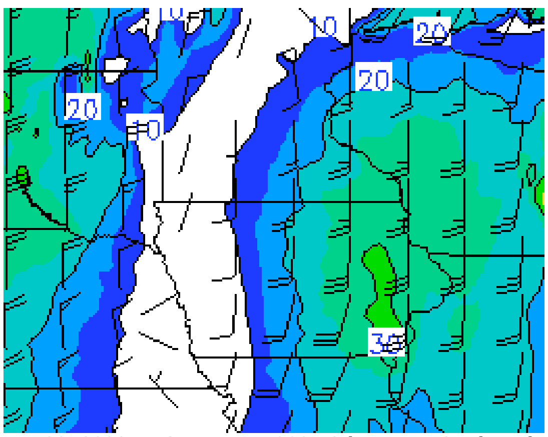

Figure 30. 2000 UTC 15 May 1968 12-km WRF 0-1 km shear magnitude and vector (kt).

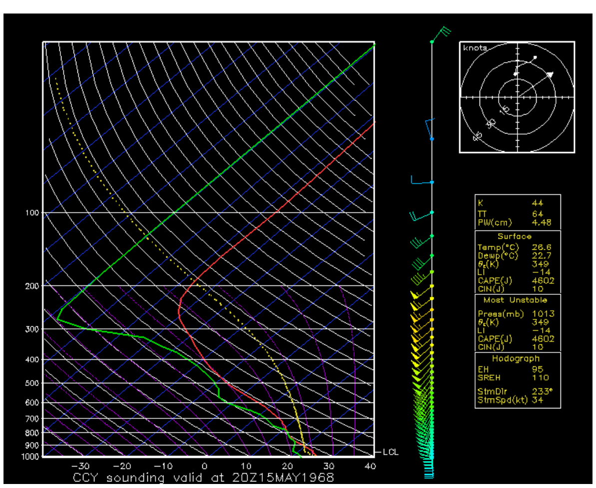

Figure 31. 8-hr forecast sounding valid at 2000 UTC 15 May 1968 for CCY (Charles City).

3.4 *13 June 1976 Jordan, IA EF-5*

It is said that Dr. Ted Fujita considered the Jordan, Iowa tornado (Fig. 32) to be the most violent he had ever studied (Grazulis, 1993). In addition to the EF-5 tornado that swept away entire farms and killed hundreds of cattle, this isolated storm also produced a well-documented anticyclonic tornado of EF-3 intensity (Brown and Knupp 1980). The tornado tracked 17 miles and injured nine people (Fig. 33).

Figure 32. Photo of the Jordan tornado near Highway 30 in central Iowa, just south of the town of Jordan. Photo by Larry Thomson.

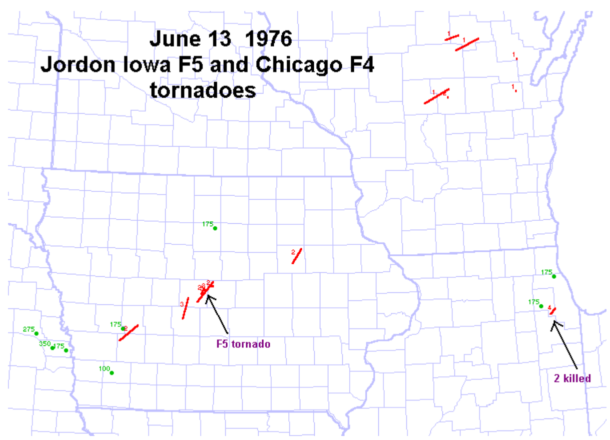

Figure 33. Plot of tornadoes on 13 June 1976 from SPC SeverePlot program. Courtesy of Jonathan Finch.

The 500-mb setup for the Jordan tornado is remarkable in its lack of a shortwave trough or speed maximum in the 500-mb flow (Fig. 34). Heights at 0000 UTC 16 May 1968 do show moderate southwesterly flow aloft. The location of the WRF ridge axis (Fig. 34b) appears to be farther east over the Dakotas than that indicated by the large-scale reanalysis (Fig 34a).

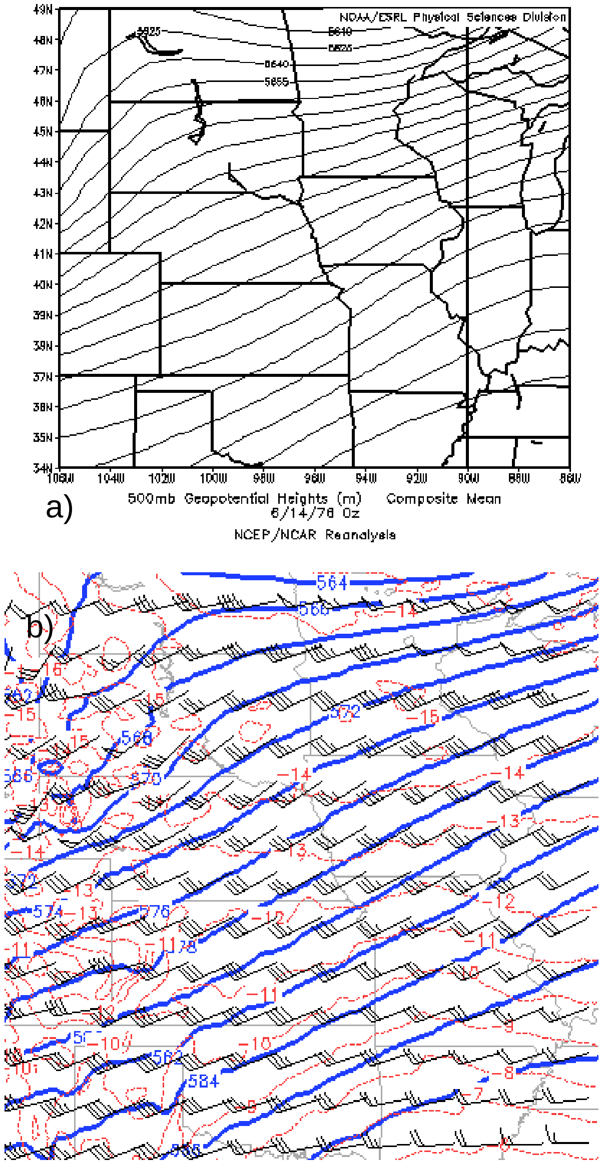

Figure 34. a) Reanalysis 500-mb height at 00 UTC 14 June 1976. b) 12-hr forecast 12-km WRF output – 500-mb height/temp/wind valid at the same time.

Figure 35a shows hand-plotted and analyzed surface map (courtesy Jonathan Finch) from 1900 UTC. This map indicates a strong dewpoint gradient across central Iowa associated with a retreating outflow boundary lifting northward across the state. Convergence and changes in the surface winds are subtle with this feature, however. The 12-km WRF output looks similar for the wind fields, but the location of the analyzed surface low is too far east, and pressures over southern Iowa are a few millibars too low. Lack of a well-defined convergence zone apparently made this event difficult to model, at least in terms of convective development (See section 2). This configuration of the WRF produced no convection for the event, although many test runs produced convection in error over northern Missouri when, in reality, a large complex of storms developed over Iowa. Without convective "contamination" however, other mesoscale fields appeared to develop reasonably in the run shown here.

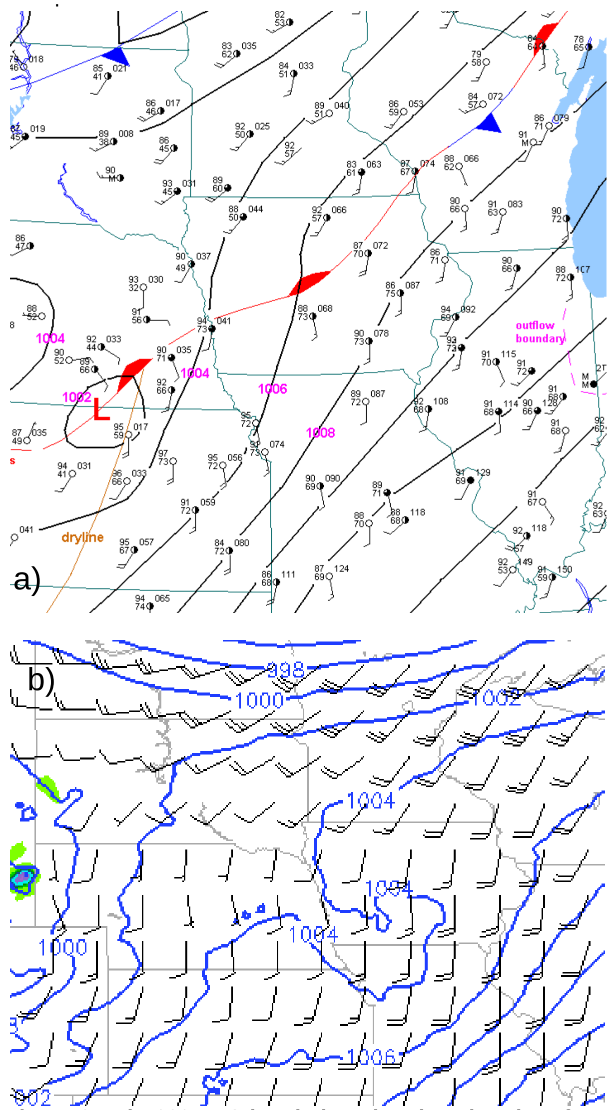

Figure 35. a) 1900 UTC hand-plotted and analyzed surface map (courtesy Jonathan Finch). b) 7-hr forecast valid at 1900 UTC 13 June 1976 12-km WRF MSLP/surface wind (kt) and 1-hr precip.

By 2000 UTC, instability built strongly into central and southeast Iowa, with a strong gradient in CAPE from southwestern into northern Iowa (Fig. 36). The CAPE gradient looks realistic given the few surface observations across Iowa at 1900 UTC (Fig. 35a). This gradient increased during the afternoon hours, as maximum CAPE values topped 4500 J kg^{-1}.

WRF 0-1 km bulk shear values were not impressive, as might be expected given the lack of detail in the low-level wind field. Values increased to near 20 kt (10 ms^{-1}) by 2000 UTC (Fig 37), however, and continued to gradually increase during the afternoon in the simulation.

WRF forecast sounding for Des Moines (DSM; Fig. 38) again shows steep full tropospheric lapse rates, strong instability, moderate deep-layer speed shear and weak to moderate directional shear.

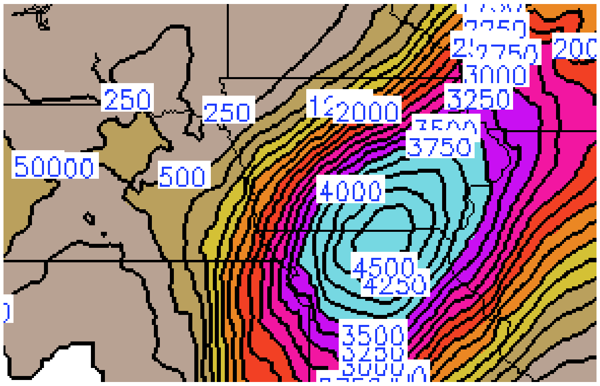

Figure 36. Surface-based CAPE from the 12-km WRF at 2000 UTC 13 June 1976.

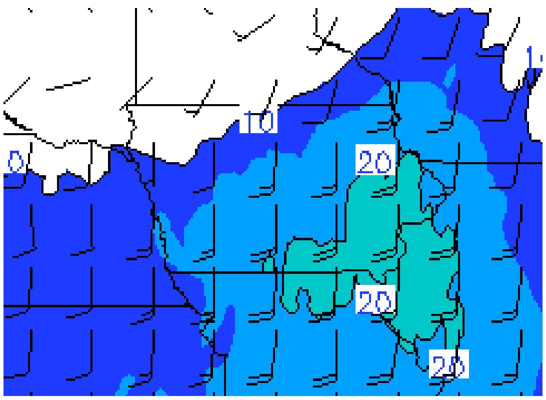

Figure 37. 2000 UTC 13 June 1976 12-km WRF 0-1 km shear magnitude and vector (kt).

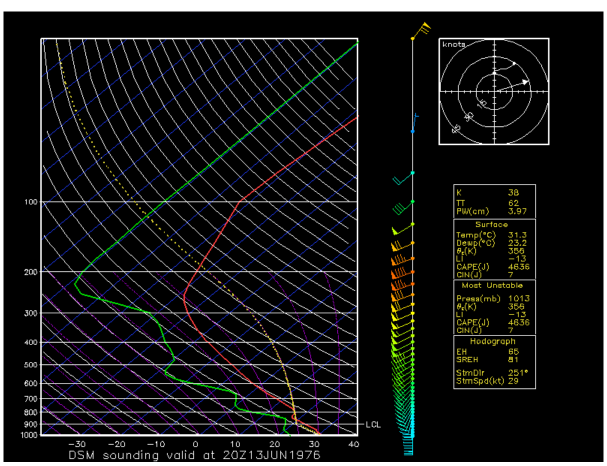

Figure 38. 8-hr forecast sounding valid at 2000 UTC 13 June 1976 for DSM (Des Moines).

3.5 *25 May 2008 Parkersburg/New Hartford, IA EF-5*

Even though this is a new case, with a myriad of mesonet, radar and model data available, it is included to illustrate the added detail obtainable when the WRF model is initialized with higher resolution 32-km NARR data. On 25 May 2008 a large and destructive EF-5 tornado tore a 43 mile long path across northeast Iowa killing eight people, injuring dozens and causing several millions of dollars worth of destruction (Figs. 39 and 40).

Figure 49. Photo of the Parkersburg tornado as it entered the west edge of town, taken by the Grundy County sheriff.

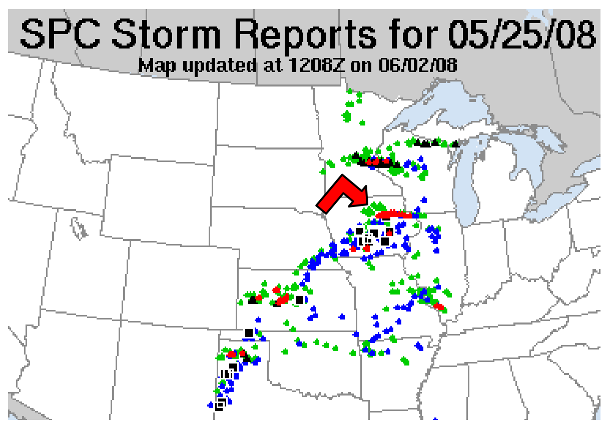

Figure 50. SPC Storm Reports plot 25 May 2008. The Parkersburg / New Hartford supercell is the west to east track (red arrow).

The 500-mb heights at 0000 UTC 26 May 2008 show strong WSW flow aloft (60-70 kt [31-36 ms^{-1}]over northeast Iowa), but any shortwave trough is well to the northwest over the Dakotas. There is good agreement between the large-scale reanalysis (Fig 51a) and the 3.5-km output from the inner nest of the WRF (Fig 51b).

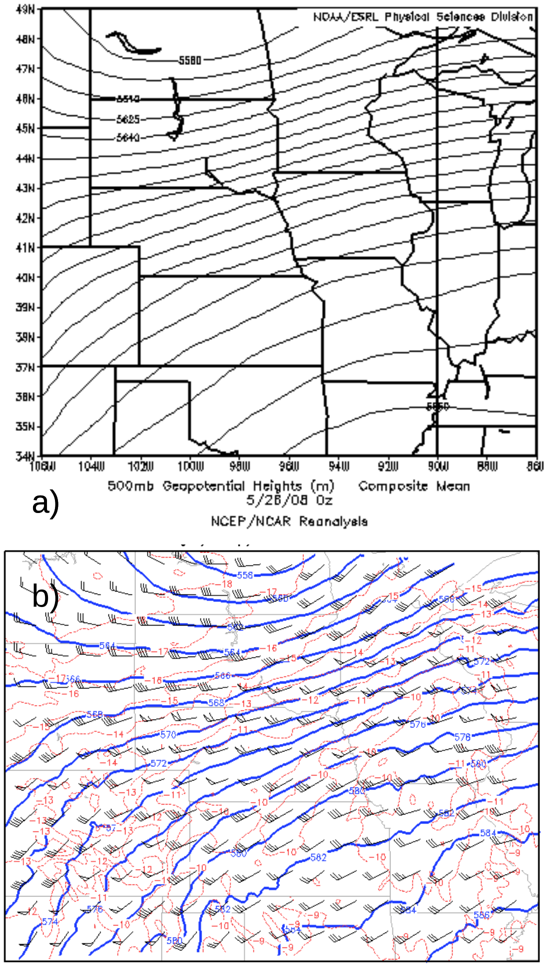

Figure 51. a) Reanalysis 500-mb height at 00 UTC 26 May 2008 b) 12-hr forecast 12-km WRF output – 500-mb height/temp/wind valid at the same time.

Figure 52 compares the combination objective/hand analyzed surface map to the WRF output. WRF output at 2100 UTC is shown because the lighter coverage of precipitation makes it easier to see the wind shift line (shaded, Fig. 52b), and its location is similar to the 2200 UTC output. Although the WRF eastward progression is a bit slow, it compares favorably to the analysis. Backed surface flow is not evident in northeast Iowa, but there is some indication in central Iowa (center of the shaded oval).

Only a limited amount of convective precipitation was generated in the WRF 3.5-km run by 2200 UTC (Fig. 56a), as compared to the observed radar reflectivity (Fig. 57). By 0000 UTC (Fig. 56b), the simulated radar reflectivity was more widespread, possibly indicating that the WRF simulation was a couple of hours slow.

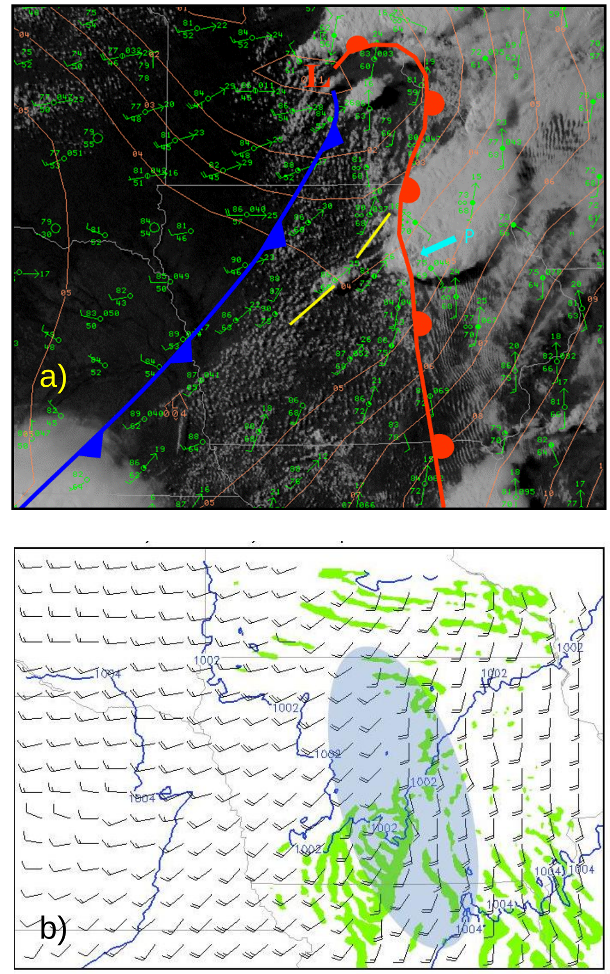

Figure 52. a) 2200 UTC 25 May 2008 visible satellite image with surface observations and fronts. The supercell that produced the Parkersburg, IA tornado is shown by the blue arrow. Note the locally backed surface winds to the east and northeast of Parkersburg. b) 9-hour forecast valid at 2100 UTC 25 May 2008 3.5-km WRF MSLP/surface wind (kt) and 1-hr precip. Wind shift axis shaded.

Surface-based CAPE can be compared to the SPC mesoanalysis data from the same time at 2200 UTC. It appears that the WRF (Fig 58a) may have placed too much CAPE northeast of the surface boundary indicated in Figure 52b. Also, the WRF may have too much drying and decrease in CAPE in north-central Iowa behind the boundary, where the SPC mesoanalysis shows a ridge of maximum CAPE (Fig. 58b). Maximum SPC CAPE is also 1000-2000 J kg^{-1} higher than the WRF CAPE.

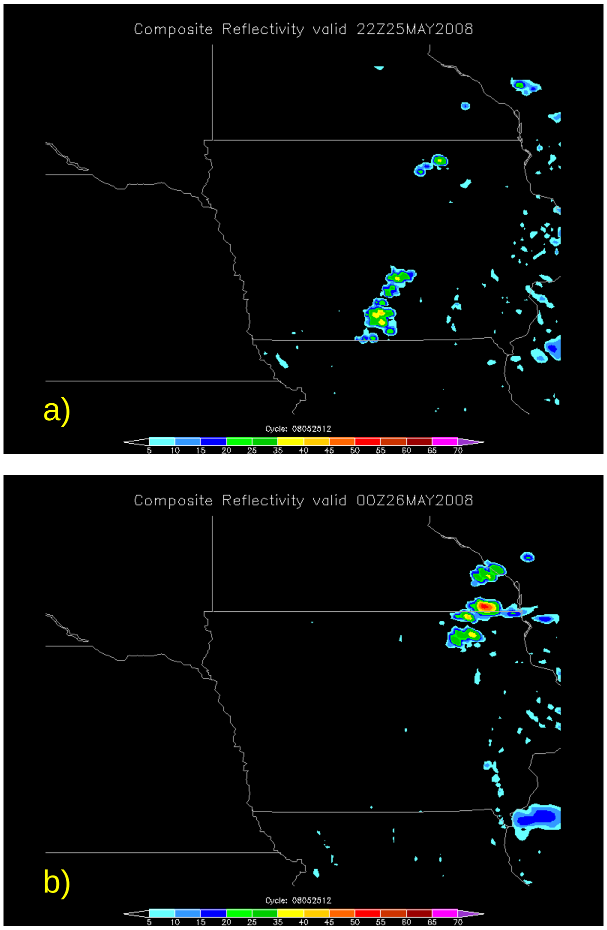

Figure 56. a) 10-hr forecast valid at 2200 UTC 25 May 2008 WRF model-simulated composite radar reflectivity. b) Same as a., except for 12-hr forecast valid at 0000 UTC on 26 May 2008.

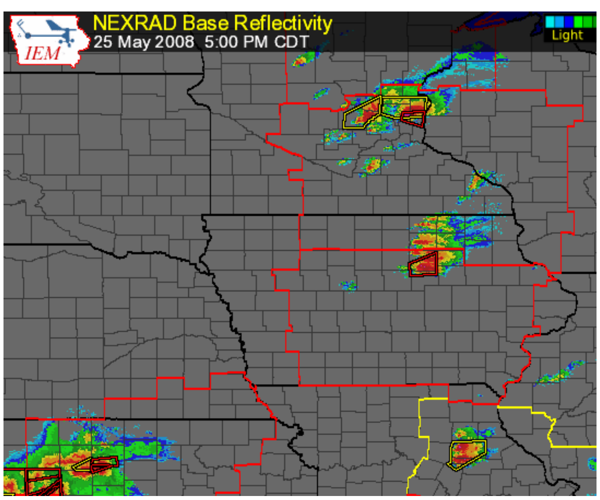

Figure 57. Observed regional composite of base reflectivity at 2200 UTC 25 May 2008. Courtesy of the Iowa Environmental Mesonet.

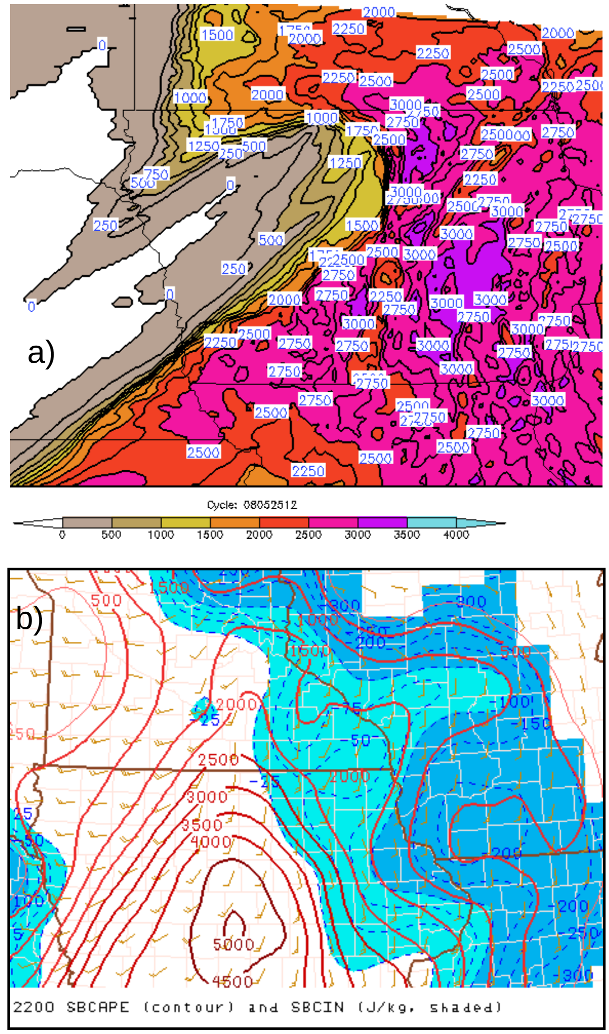

Figure 58. a) 8-hr forecast of surface-based CAPE (J kg^{-1}) from the 12-km WRF valid at 2000 UTC 15 May 1968. B) SPC mesoanalysis valid at the same time.

WRF 0-1 km bulk shear values (Fig. 59a) are slightly higher, with some exceeding 30 kt (26 ms^{-1}), than the SPC mesoanalysis of 0-1km shear (Fig. 59b). What is more significant, however, is that the general location of the maximum values appear to be several counties too far south in the WRF simulation.

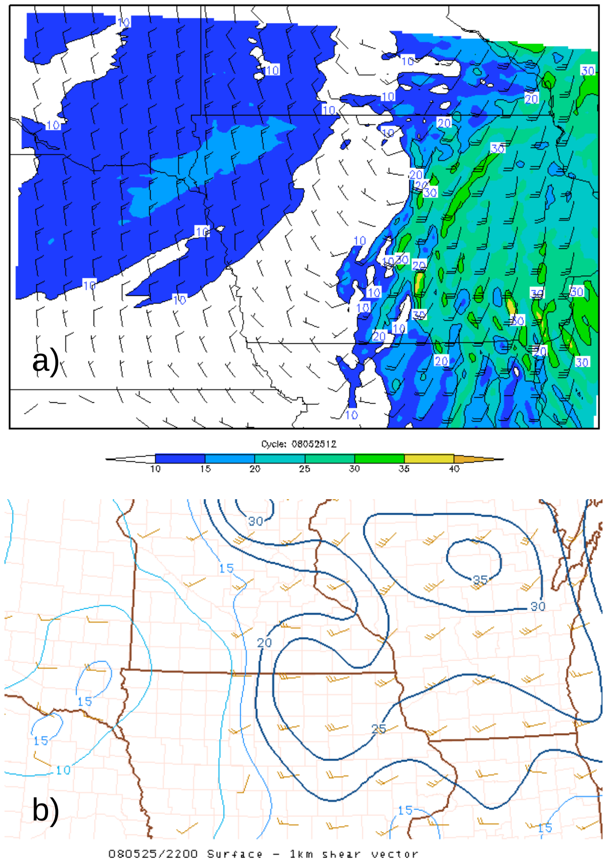

Figure 59. a) 10-hr forecast valid at 2200 UTC 25 May 2008 3.5-km WRF 0-1 km shear magnitude and vector (kt). b) SPC mesoanalysis of 0-1 km shear at the same time.

The WRF forecast sounding for Waterloo (ALO; Fig. 60) compares favorably to the 00-hr RUC analysis sounding at 2200 UTC. It appears that the WRF has a slightly steeper lapse rate below 700-mb, but CAPE is similar in the two soundings. The RUC analysis sounding shows stronger veering of the winds in low levels, but the WRF forecast appears from the hodographs to have stronger low-level winds in the lowest 1-2 km. Again, lapse rates are steep, but not as much so as some of the other EF-5 cases shown in this study.

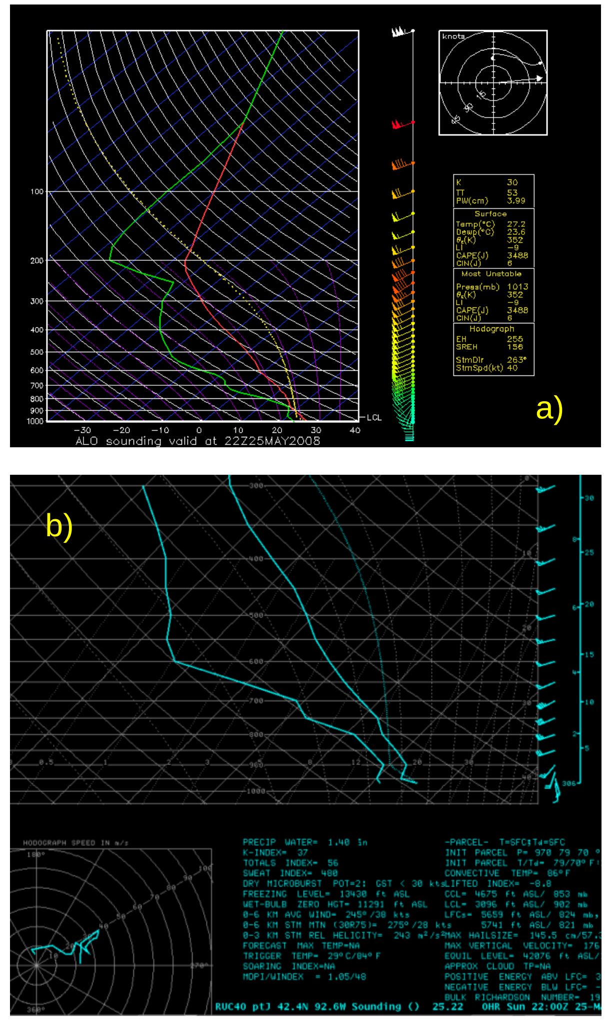

Figure 60. a) 10-hr forecast sounding valid at 2200 UTC 25 May 2008 3.5-km WRF for ALO. b) RUC 00-hr analysis sounding for ALO valid at the same time.

3.6 *28 June 1979 Manson, IA EF-4*

The 28 June 1979 Manson / Algona, Iowa tornadoes were also modeled here. An EF-4 tornado killed three in Manson, while an EF-3 tornado killed two and injured 34 in Algona. According to Waite and Weinbrecht (1980), this was one of the greatest northwest flow tornado outbreaks in history (Fig. 61). In addition, Johns (1979) considered this to be a particularly challenging forecast event, due to the rapid intensification and evolution of the weather system. A surface map from the Johns (1979) paper at 0000 UTC on 29 June 1979 shows an intricate convergence of moisture discontinuities, outflow boundaries, wind shift lines and fronts near the location and time of the tornadoes in northern Iowa (Fig. 62).

Figure 63 shows the 3.5-km WRF surface simulation of the situation, and it appears to compare favorably with the Johns analysis. Some detail in the surface wind pattern may also be captured by the WRF simulation. Specific comparisons will be left to the reader.

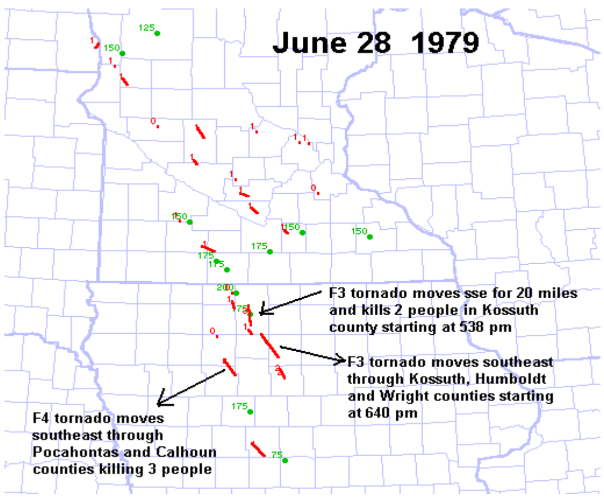

Figure 61. Plot of tornadoes on 28 June 1979 from SPC SeverePlot program. Courtesy of Jonathan Finch.

The WRF simulation also depicts a narrow axis of stronger instability ahead of the convective activity extending from northwest Iowa into southern Minnesota (Fig. 64). The density of the surface observation network in 1979 may not have been of sufficient density to determine if this depiction is accurate.

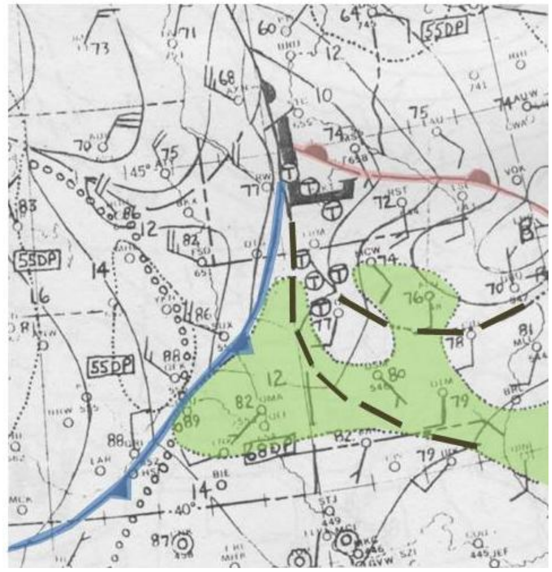

Figure 62. Color-enhanced surface analysis from the Johns (1979) paper, 0000 UTC 29 June 1979. Tornado locations are indicated by the circled "T". Surface dewpoints in excess of 68 deg F are shaded in green.

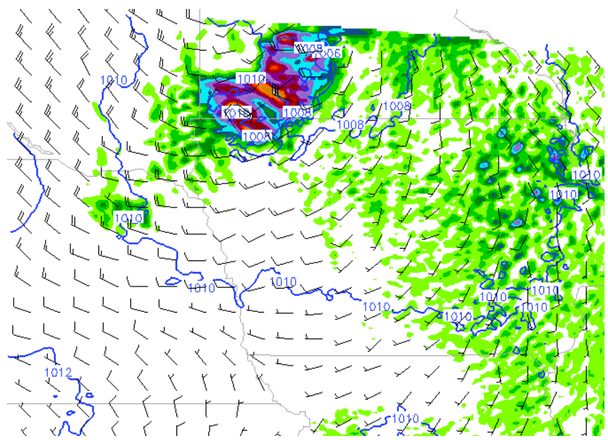

Figure 63. 11-hr forecast valid at 2300 UTC 28 June 1979 3.5-km WRF MSLP/surface wind (kt) and 1-hr precip.

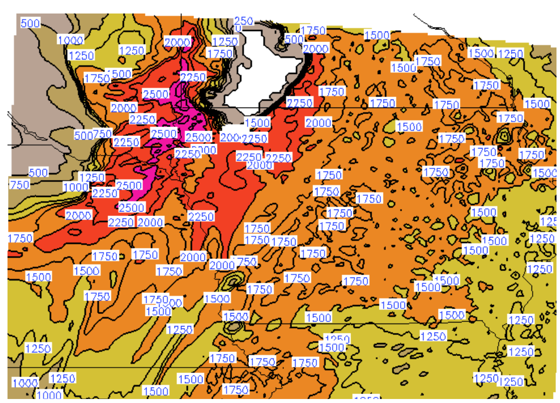

Figure 64. 11-hr forecast valid at 2300 UTC 28 June 1979 3.5-km WRF surface-based CAPE (J kg^{-1}).

Values of 0-1 km shear were quite weak in the WRF simulation (Fig. 60). Johns (1979) also mentioned weak low-level flow, so this would appear to be an accurate forecast.

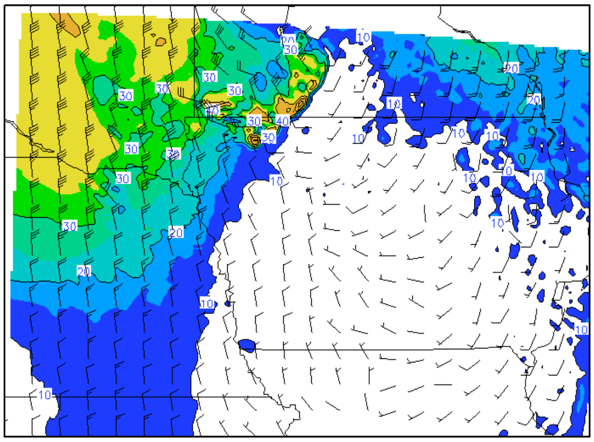

Figure 65. 2300 UTC 28 June 1979 3.5-km WRF 0-1 km shear magnitude and vector (kt).

Finally, WRF simulated radar reflectivity for 0000 UTC 29 June 1979 (Fig. 66) shows a reasonable convective structure and configuration, that would have been useful to forecasters in 1979, and similar output should be useful today.

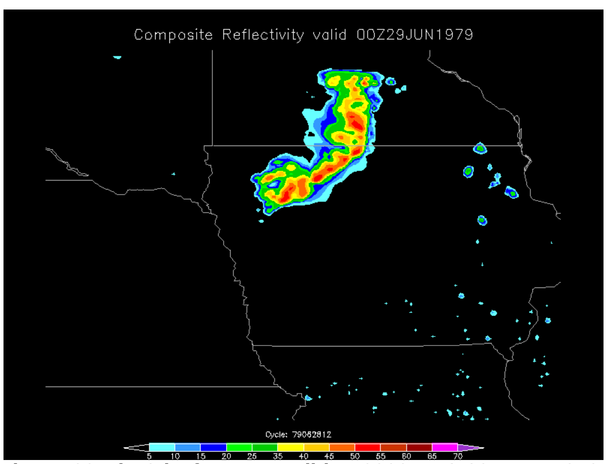

Figure 66. a) 12-hr forecast valid at 0000 UTC 29 June 1979 WRF model-simulated composite radar reflectivity.

4. ENVIRONMENTS OF IOWA'S EF-5 TORNADOES – LESSONS LEARNED

Of the EF-5 tornado events, two fit the classic warm season tornado outbreak pattern identified in local studies at the National Weather Service in Des Moines (Figs. 1 and 2). Both the 1966 and 1968 events had strong surface low pressure centers, and a strong progressive short wave trough aloft. The 1953 and 2008 events were more subtle, occurring farther south of the mid to upper level jet maxima, and with less proximity to the main surface low pressure center. The 1976 Jordan tornado occurred with the weakest forcing, and no short wave could be identified in the west-southwest flow aloft. In addition, it occurred along a somewhat weakly defined boundary, and a weak surface low pressure center on that boundary was several hundred kilometers to the southwest of the tornado development. This indicates that there is knowledge to be gained, especially by learning details of the less classic events.

Four of the six EF-4 tornado events fit the classic outbreak pattern, possibly because these cases were chosen for noteworthy EF-4 tornadoes and high outbreak rankings. Still, two of the events, 1979 and 1974, were northwest flow cases where the surface pressure pattern was less well-defined compared to the classic pattern.

All told, three, to as many as five of the eleven cases did not match the classic Iowa outbreak pattern. Did the WRF model simulations illuminate subtleties that made these events particularly damaging? The answer for the pre-1979 NNRP initialized cases, appears to be no. In the 1976 and 1953 EF-5 cases, and to some extent, the 1968 Charles City EF-5, surface plots and hand analysis strongly suggest that low-level outflow boundaries played a key role. Due to the extremely course initialization data set, numerous model runs often gave no indication of these boundaries. As a result, simulated low-level wind shear was often well below what would have been expected given the available surface wind observations. In addition, CAPE and buoyancy gradients were weak, even in the presence of strong CAPE, when one would expect significant gradients across the boundaries.

Still, one can get a feel for the evolving environment using the WRF simulations, in a way that is not possible by simply looking at 1200 and 0000 UTC RAOB data and a few surface plots. This is especially true when viewing hourly data, changes and animations of the output. Instability often evolved rapidly, with destabilization allowing high values of CAPE to arrive just in time for the tornado event. This is to be expected in dynamic events, and the WRF simulations concurred, even in some of the less strongly forced events.

Another commonality that struck this author was the steep mid-level lapse rates indicated by WRF soundings for a vast majority of these events. This, combined with low-level thermal and moisture profiles in balance with the mid-levels, prevented prohibitive capping. It also produced moderate to strong low-level buoyancy, and resulted in deep full tropospheric lapse rates in most cases. Thus the old adage, "beware the loaded gun", still applies even in less than classic synoptic setups.

The post-1979 NARR-initialized cases appeared more realistic, as might be expected. Evolution of shear and CAPE, as simulated by the WRF, matched reality much better than in the older cases. This is not to say, however, that simulations were nearing perfection. For the 2008 Parkersburg case, for example, a realistic looking north-south boundary was developed in the model. But this boundary was too far west and slow in progression, and no convection developed in vicinity of the tornado location throughout the 12-hour simulation. In some cases, modeled convection contained subtle features that were exhibited in observations. Compare, for example, Figure 67, where a break in the convection over southern Iowa was captured by the WRF.

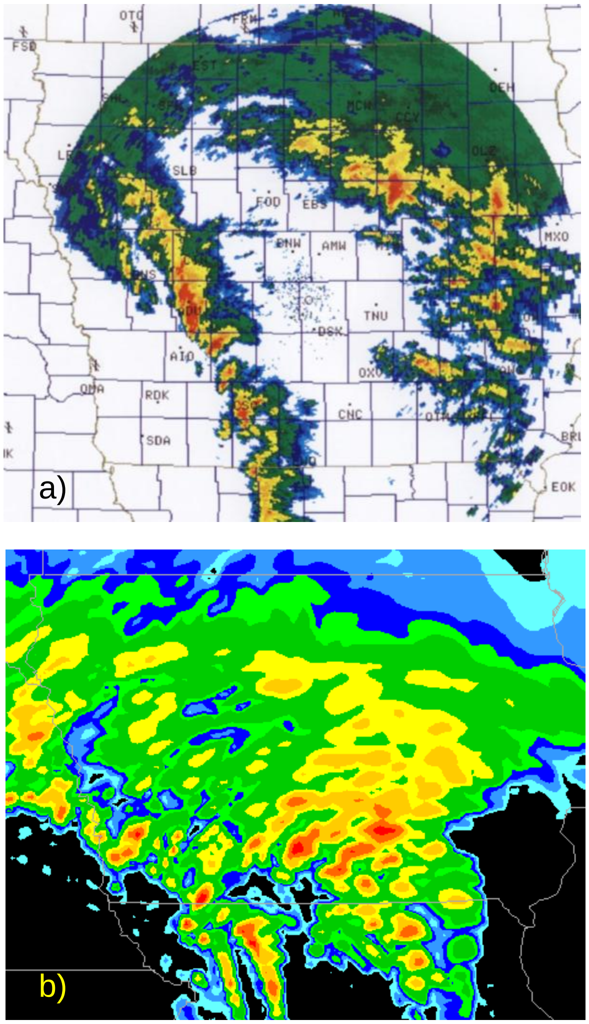

Figure 67. a) WSR-88D reflectivity at 2036 UTC on 8 April 1999. b) 9-hr forecast valid at 2100 UTC 8 April 1999 WRF model simulated composite radar reflectivity.

5. CONCLUSIONS

Based upon the qualitative evaluations undertaken for this conference presentation, it is possible to deepen the understanding of EF-5 tornado events using the WRF model, and reanalysis data for initialization. Use of post-1979 regional reanalysis (NARR) data is more satisfying in this regard, when compared to the lower resolution pre-1979 global reanalysis (NNRP) for initialization. WRF runs, even when nested down to a 3.5-km grid from the NNRP, simply cannot resolve low-level boundaries, buoyancy gradients and backed low-level winds that are critical to high-end tornado environments. As a result, values of 0-1 km shear, for example, appear to be much lower than expected when looking at surface plots. Therefore, it is *not* recommended that climatologies of hodographs, helicity or low-level shear profiles be built from similar historical WRF runs.

In general, the same can be said for thermodynamic variables, although it is clear that steep low-level and mid-level lapse rates were present in many of these events, as well as relatively low LCL heights (not shown). One simply should not build a proximity sounding from the WRF historical "forecast" output, since too many details of the sounding could be misplaced in the simulation. Several of the post-1979 NARR simulations showed promise, however, with development of realistic boundaries and convective organization.

On a positive note, it is useful to loop WRF output of numerous variables to get a general understanding of how these historic EF-5 events evolved. CAPE often changed dramatically in the hours leading up to the tornado time, reinforcing the sound practice of continually re-evaluating convective environmental trends, especially (obviously) on those days with a loaded gun sounding. Although low-level shear did not appear to be well simulated by the WRF, it was interesting to see that many of the historic tornadoes occurred on the trailing edge of a region of extremely high shear.

Some examples of loops of WRF output from EF-5 cases in this paper can be found at this link: http://www.crh.noaa.gov/dmx/?n=sls2008jungbluth

To reverse or solidify these qualitative observations would take a considerable amount of work and a longer list of cases. It would be useful to directly compare forecast WRF soundings to RAOB soundings at 0000 UTC. However, as with many studies of proximity soundings, it is always difficult to find RAOB soundings truly representative of the near-storm environment, and this is complicated by the effects of convection within the WRF.

Finally, forecasters gather a lot of information from depictions of simulated reflectivity in today's semi-operational high resolution WRF forecasts. This includes suggestions of convective mode, timing and evolution, all of which were not addressed in any depth here. Microfilm of radar imagery from these historic events has been ordered, and it would be interesting to see if the WRF simulations approach the structure of the actual convection, especially for pre-WSR-88D events. If the WRF shows value in these historic re-creations, then it would also be of value in day-to-day use.

6. ACKNOWLEDGEMENTS

The author would like to thank Shane Searcy, Information Technology Officer at the NWS in Des Moines for many hours of technical assistance, and encouragement with this project. Rob Rozumalski, NWS National SOO Science and Training Resource Coordinator, is to be thanked for his dedication toward making the WRF available for use by the common man. Adam Clark and William Gallus at Iowa State University also provided expertise and assistance with WRF configuration and GrADS output scripts.

7. REFERENCES

Aligo E. A., W. A. Gallus Jr., and M. Segal, 2008: On the Impact of WRF Model Vertical Grid Resolution on Midwest Summer Rainfall Forecasts. *Wea. Forecasting,* in press.

Brown, J. M., and K. R. Knupp, 1980: The Iowa Cyclonic-Anticyclonic Tornado Pair and Its Parent Thunderstorm. *Mon. Wea. Rev.*, **108**, 1626–1646.

Jankov I., W.A. Gallus Jr., M. Segal, B. Shaw, and S. E. Koch, 2005: The Impact of Different WRF Model Physical Parameterizations and Their Interactions on Warm Season MCS Rainfall. *Wea. Forecasting*, **20**, 1048-1060.

Gallus W. A. Jr., and J. F. Bresch, 2006: Comparison of Impacts of WRF Dynamic core, Physics Package, and Initial Conditions on Warm Season Rainfall Forecasts. *Mon. Wea. Rev.*, **134**, 2632–2641.

Grazulis, T. P., 1993: *Significant Tornadoes 1680-1991*. Environmental Films, St. Johnsbury, VT, 1326 pp.

Johns, R. H., 1979: The Severe Thunderstorm Outbreak fo June 28 and 29, 1979. Technical Attachment 79-10, 7 pp. [Available from NOAA/NWS Central Region Headquarters Regional Office, 7220 NW 101st Terrace, Kansas City, MO 64153]

Kain, J. S., and J. M. Fritsch,1993: Convective parameterization for mesoscale models: The Kain–Fritsch scheme. *The Representation of Cumulus Convection in Numerical Models, Meteor. Monogr.,* No. 46, Amer. Meteor. Soc., 165–170.

Lin, Y.L., R.D. Farley, and H.D. Orville, 1983: Bulk Parameterization of the Snow Field in a Cloud Model. *J. Appl. Meteor.*, **22**, 1065–1092.

Marshall, T. P., K. A. Jungbluth and A. Baca, 2008: The Parkersburg, IA Tornado: 25 May 2008. *24th Conference on Severe Local Storms*, Savannah, GA, Amer. Meteor. Soc., P3.3.

Mesinger, F., G. DiMego, E. Kalnay, K. Mitchell, P.C. Shafran, W. Ebisuzaki, D. Jovic, J. Woollen, E. Rogers, E.H. Berbery, M.B. Ek, Y. Fan, R. Grumbine, W. Higgins, H. Li, Y. Lin, G. Manikin, D. Parrish, and W. Shi, 2006: North American Regional Reanalysis. *Bull. Amer. Meteor. Soc.*, **87**, 343–360.

National Weather Service, cited 2006: WRF Environmental Modeling System User's Guide. [Available online at http://strc.comet.ucar.edu/wrf/wrf_userguide.htm.]

Skamarock, W. C., J. B. Klemp, J. Dudhia, D. O. Gill, D. M. Barker, W. Wang, J. G. Powers, 2005: A description of the Advanced Research WRF Version 2. NCAR Technical note NCAR/TN-468 + STR, 88 pp.

Thompson, R.L. and M.D. Vescio, 1998: The Destruction Potential Index: A Method for Comparing Tornado Days. Preprints, *19th Conf. Severe Local Storms*, Minneapolis MN, Amer. Meteor. Soc., 280-286.

Kistler, R., E. Kalnay, W. Collins, S. Saha, G. White, J. Woollen, M. Chelliah, W. Ebisuzaki, M. Kanamitsu, V. Kousky, H. van den Dool, R. Jenne, M. Fiorino, 2001: The NCEP-NCAR 50-Year Reanalysis: Monthly Means CD-ROM and Documentation. *Bull. Amer. Meteor. Soc.,* ***82,*** *247-268.*

Warner, T. T., and H.-M. Hsu, 2000: Nested-model simulation of moist convection: The impact of coarse-grid parameterized convection on fine-grid resolved convection. *Mon. Wea. Rev.,* **128,** 2211–2231.

Waite, P., C. Winbrecht, 1980: An Upper Midwest Tornado Outbreak on 28 June 1979. *NWA Digest*, **5**, 63-68.

WSEC (Eds.), 2006: A recommendation for an enhanced Fujita scale (EF-scale). Wind Science and Engineering Center, Texas Tech University, Lubbock, Texas, 95 pp. [Available at http://www.wind.ttu.edu/EFScale.pdf]